Eradication of Solid Human Breast Tumors in Nude Mice with an Intravenously Injected Light-Emitting Oncolytic Vaccinia Virus

Qian Zhang,[1] Yong A. Yu,[1] Ena Wang,[2] Nanhai Chen,[1] Robert L. Danner,[3] Peter J. Munson,[4] Francesco M. Marincola,[2] and Aladar A. Szalay[1,5]

[1]Genelux Corporation, San Diego Science Center, San Diego, California; [2]Immunogenetics Laboratory, Department of Transfusion Medicine; [3]Functional Genomics and Proteomics Facility, Critical Care Medicine Department, Clinical Center; [4]Mathematical and Statistical Computing Laboratory, Division of Computational Bioscience, Center for Information Technology, NIH, Bethesda, Maryland; and [5]Virchow Center for Experimental Biomedicine, Institute for Biochemistry and Institute for Molecular Infection Biology, University of Würzburg, Am Hubland, Würzburg, Germany

Abstract

Previously, we reported that a recombinant vaccinia virus (VACV) carrying a light-emitting fusion gene enters, replicates in, and reveals the locations of tumors in mice. A new recombinant VACV, GLV-1h68, as a simultaneous diagnostic and therapeutic agent, was constructed by inserting three expression cassettes (encoding *Renilla* luciferase–*Aequorea* green fluorescent protein fusion, β-galactosidase, and β-glucuronidase) into the *F14.5L*, *J2R* (encoding thymidine kinase) and *A56R* (encoding hemagglutinin) loci of the viral genome, respectively. I.v. injections of GLV-1h68 (1×10^7 plaque-forming unit per mouse) into nude mice with established (~300–500 mm^3) s.c. GI-101A human breast tumors were used to evaluate its toxicity, tumor targeting specificity, and oncolytic efficacy. GLV-1h68 showed an enhanced tumor targeting specificity and much reduced toxicity compared with its parental LIVP strains. The tumors colonized by GLV-1h68 exhibited growth, inhibition, and regression phases followed by tumor eradication within 130 days in 95% of the mice tested. Tumor regression in live animals was monitored in real time based on decreasing light emission, hence demonstrating the concept of a combined oncolytic virus–mediated tumor diagnosis and therapy system. Transcriptional profiling of regressing tumors based on a mouse-specific platform revealed gene expression signatures consistent with immune defense activation, inclusive of IFN-stimulated genes (*STAT-1* and *IRF-7*), cytokines, chemokines, and innate immune effector function. These findings suggest that immune activation may combine with viral oncolysis to induce tumor eradication in this model, providing a novel perspective for the design of oncolytic viral therapies for human cancers. [Cancer Res 2007;67(20):10038–46]

Introduction

Numerous reports have confirmed that intratumoral injection of various viruses can result in virus replication in tumors, followed by oncolysis of tumor cells (1, 2). More recent findings support the notion that, upon systemic delivery, both DNA and RNA viruses are capable of entering, replicating, and persisting in established tumors. Attenuated adenovirus ONYX-015, when delivered intravenously has been shown to enter and replicate in subcutaneous and intraparenchymal tumor xenografts (3). Likewise, a live attenuated Edmonston-B strain of measles virus replicates in large established human lymphoma xenografts and interferes with tumor growth post i.v. injection (4). Furthermore, naturally occurring variants of vesicular stomatitis virus, when delivered systemically, replicates in human ovarian xenografts, causing tumor size reduction in immunocompetent mice (5). Additional examples of systemically delivered viruses with antitumor activity include Newcastle disease virus (6, 7), reovirus (8, 9), lentivirus (10), herpes simplex virus (11, 12), enterovirus (13), Sindbis virus (14), and Semliki Forest virus (15). Similar observations of tumor targeting and therapy were also reported using systemically delivered bacteria (16, 17).

Due to the large size of its genome, vaccinia virus (VACV) is particularly attractive as a potential antitumor agent. Cytoplasmically replicating wild-type (wt) and mutant VACVs also show tumor-specific entry and replication upon systemic delivery. Deletional mutations introduced into nonessential genes, such as *J2R* [encoding thymidine kinase (TK); refs. 18, 19], *A56R* (encoding hemagglutinin; ref. 20), and vaccinia growth factor (VGF) gene (19) of the viral genome, resulted in significant attenuation of wt Western Reserve (WR) strain. Intraperitoneal delivery of the TK^- and VGF^- viral strain shows growth retardation of tumors in mice (19). Additionally, foreign genes encoding tumor suppressor proteins, immunostimulatory proteins, and cytokines, as well as pro–drug-activating enzymes, have been inserted into the nonessential loci of VACV genome for therapy of tumors (21–23).

In addition to its therapeutic potential, VACV has also been studied as a gene delivery tool for tumor detection. Previously, we have visualized in real time the translocation and distribution of a recombinant VACV in tumorous mice. Due to tumor-specific replication and the expression of light-emitting proteins by the virus, the location of tumors and metastases were revealed by optical imaging (24). The expression of the VACV (WR strain)–encoded somatostatin receptor in tumors has been tested as a method to bind radiolabeled ligands for the detection of tumors in mice using positron emission tomography (25).

In this paper, we describe the construction and characterization of a new recombinant VACV (LIVP strain), GLV-1h68, and show its function as a simultaneous diagnostic and, most importantly, as a therapeutic agent. GLV-1h68 was constructed by inserting three expression cassettes [*Renilla* luciferase–*Aequorea* green fluorescent

Note: Supplementary data for this article are available at Cancer Research Online (http://cancerres.aacrjournals.org/).

Q. Zhang and Y. Yu contributed equally to this work.

The microarray data discussed in this publication have been deposited in National Center for Biotechnology Information Gene Expression Omnibus (GEO; http://www.ncbi.nlm.nih.gov/geo/) and are accessible through GEO series accession number GSE8513.

Requests for reprints: Aladar A. Szalay, Genelux Corporation, San Diego Science Center, 3030 Bunker Hill Street, San Diego, CA 92109. Phone: 858-483-0024; Fax: 858-483-0025; E-mail: aaszalay@genelux.com.

doi:10.1158/0008-5472.CAN-07-0146

protein (RUC-GFP) fusion, β-galactosidase, and β-glucuronidase] into the *F14.5L, J2R*, and *A56R* loci of the viral genome, respectively. The recombinant GLV-1h68 virus was subsequently injected i.v. into human breast GI-101A tumor-bearing nude mice for characterizing its tumor targeting and replication capability and its toxicity. Furthermore, the effect of tumor colonization by GLV-1h68 on growth, regression, and eradication of tumors without the need for therapeutic transgenes was also investigated. Tumor regression in live animals was monitored in real time based on decreasing light emission, thereby demonstrating the concept of a combined oncolytic virus–mediated tumor diagnosis and therapy system. Species-specific transcriptional profiling was applied to evaluate the host contribution in the process of tumor regression.

Materials and Methods

Cell lines. African green monkey kidney fibroblasts (CV-1) were obtained from the American Type Culture Collection (ATCC). Cells were cultured in DMEM supplemented with antibiotic-antimycotic solution (100 U/mL penicillin G, 250 ng/mL amphotericin B, 100 units/mL streptomycin) and 10% fetal bovine serum (FBS; Invitrogen Corporation) at 37°C under 5% CO_2. Cell line GI-101A (kindly provided by Dr. A. Aller, Rumbaugh-Goodwin Institute for Cancer Research, Inc.), a highly metastatic derivative of GI-101 human ductal adenocarcinoma (26), was cultured in RPMI 1640 supplemented with 5 ng/mL β-estradiol and 5 ng/mL progesterone (Sigma), 10 mmol/L HEPES, 1 mmol/L sodium pyruvate, 20% FBS, and antibiotic-antimycotic solution (all reagents except noted were supplied by Mediatech, Inc.). Mouse embryonic fibroblasts MEF (CF-1) were originally obtained from ATCC and cultured in DMEM with 15% FBS.

Plasmid DNA and virus construction. All cloning steps were done using vaccinia DNA homology-based shuttle plasmids generated for homologous recombination of foreign genes into one of the target loci in the VACV genome through double reciprocal crossover. In a previous study, a RUC-GFP fusion gene was inserted into a NotI site in the LIVP genome to generate a recombinant virus, rVV-RG, for visualization of VACV infection (27). This NotI site is located within a small open reading frame (ORF) between the *F14L* and *F15L* loci in the genome of VACV, thus named *F14.5L*. Based on sequence analysis, ORF *F14.5L* encodes a short polypeptide of 49 amino acids, which was found to be highly conserved among different vaccinia strains, as well as other poxviruses.[6]

Plasmid pSC65 (28) and pVY6 (29) were used to direct the insertions into the *J2R* and *A56R* loci of the LIVP genome, respectively. The human transferrin receptor encoding cDNA (TFR) was excised from pCDTR1 (ATCC), and cloned into pSC65 for generating the shuttle vector for insertion of β-galactosidase (*lacZ*) and TFR genes into the *J2R* locus. The TFR cDNA was inserted in the reverse orientation to vaccinia synthetic early/late promoter to serve as a negative control for a TFR-expressing recombinant virus. As a result, TFR was not expressed (data not shown). The double mutant virus GLV-1f65, therefore, carried a *lacZ* gene and a reverse TFR cDNA in the *J2R* locus, plus the RUC-GFP fusion gene in the *F14.5L* locus. To generate the triple mutant virus GLV-1h68, the *lacZ* gene in pVY6 was exchanged with the cDNA of β-glucuronidase (*gusA*), excised from pLacGUS (Invitrogen Corporation, Carlsbad, CA), and the resulting plasmid was used as the shuttle vector for insertion of gusA into the *A56R* locus. Because the *J2R* and *A56R* homologous flanking regions in the shuttle vectors pSC65 and pVY6 were of WR origin, upon recombination into wt LIVP genome, the corresponding regions in the LIVP derivatives were replaced by the highly homologous WR sequences.

Recombinant viruses were generated by transformation of shuttle plasmid vectors using the FuGENE 6 transfection reagent (Roche Applied Science) into CV-1 cells, which were preinfected with the LIVP parental virus or one of its mutant derivatives. The expression of RUC-GFP fusion protein by the recombinant viruses was confirmed by luminescence assay and fluorescence microscopy. Expressions of β-galactosidase and β-glucuronidase A were confirmed by blue plaque formation upon addition of 5-bromo-4-chloro-3-indolyl-β-D-galactopyranoside (X-gal, Stratagene) and 5-bromo-4-chloro-3-indolyl-β-D-glucuronic acid (X-GlcA, Research Product International Corporation), respectively. Positive plaques formed by the recombinant virus were isolated and purified. The clonal purity of each mutant virus isolate was verified by expression of the corresponding marker gene(s) in the *F14.5L, J2R*, and *A56R* loci, which was also confirmed by PCR and DNA sequencing. Viruses were propagated in CV-1 cells, and up to 7×10^9 plaque-forming unit (pfu)/mL of GLV-1h68 could be purified from 2×10^8 infected CV-1 cells through sucrose gradients (30).

Viral replication in cell cultures. CV-1 (1×10^5) and GI-101A (4×10^5) cells were seeded onto 24-well plates, and MEF (CF-1) (1.1×10^5) cells were seeded onto 12-well plates. After 24 h in culture, the cells were infected with individual viruses at MOI of 0.001 (for CV-1 or GI-101A cells) or MOI of 0.01 (for MEF cells). The cells were incubated at 37°C for 1 h with brief agitation every 10 min to allow infection to occur. The infection medium was removed, and cells were incubated in fresh growth medium until cell harvest at 24, 48, 72, or 96 h after infection. Viral particles from the infected cells were released by a quick freeze-thaw cycle, and the titers determined as medium (pfu/mL) in duplicate by plaque assay in CV-1 cell monolayers. The same procedure was followed using a resting CV-1 cell culture, which was obtained by culturing a confluent monolayer of CV-1 cells for 6 days in DMEM supplemented with 5% FBS before viral infection.

Toxicity and survival studies. All mice were cared for and maintained in accordance with animal welfare regulations under an approved protocol by the Institutional Animal Care and Use Committee of LAB Research International, Inc.

A total of 68 mice with GI-101A xenograft tumors were developed to assess the biodistribution and toxicity of individual viruses. Tumors were generated by implanting GI-101A cells (5×10^6 in 100 μL PBS) s.c. on the right hind leg into 6- to 8-week-old female nude mice (NCI/Hsd/Athymic Nude-*Foxn1*^{nu}, Harlan). Tumor growth was recorded twice weekly in three dimensions using a digital caliper. Tumor volume was calculated as [(length × width × height)/2] and reported in cube millimeter. On day 30 after cell implantation (tumor volume, ~300–500 mm^3), a single i.v. inoculation of individual viruses (1×10^7 pfu in 100 μL PBS) was delivered. Animals were observed daily for any sign of toxicity, and body weight was checked twice weekly. Fourteen days post–virus injection, four animals from each group were killed for analysis of viral distribution. The tumors and organs were excised, weighted, inspected, and homogenized using MagNA Lyser (Roche Diagnostics) at a speed of 6500 for 30 s. After three cycles of freeze and thaw, the supernatants were collected by centrifugation at $1000 \times g$ for 5 min. The viral titers were determined in duplicate by standard plaque assays using CV-1 cells.

The remaining mice ($n = 8$) for each group were followed up to 130 days to determine survival. Both body weights and tumor volumes were monitored continuously, and the animals were euthanized when tumors reached a volume of 4000 mm^3 or their body weight loss exceeded 50%.

Virotherapy of GI-101A xenografts with GLV-1h68. To assess growth of GI-101A tumors in nude mice upon colonization with GLV-1h68, three different doses of the virus were injected systemically via different routes. Thirty days after subcutaneous tumor cell implantation, a single dose of GLV-1h68 at 1×10^5, 1×10^6, or 1×10^7 pfu in 100 μL PBS was injected via the left femoral vein or at 1×10^6 pfu in 100 μL PBS via the tail vein. A total of 25 mice, five for each dosing group, were included in this study. Tumor measurements were recorded twice weekly for 130 days after initial virus injection, in parallel with fluorescence imaging of tumors. Six extra mice were included for the 1×10^7 pfu dosing group, allowing tumor tissues to be collected at 14, 28, and 56 days after GLV-1h68 injections for immunohistochemical analysis of β-galactosidase in 5-μm paraffin embedded tissue sections.

Gene profiling analysis on Affymetrix mouse oligoarrays. To evaluate the involvement of host mechanisms in the eradication of transplanted xenografts, we implanted human GI-101A cells (5×10^6 in 100 μL PBS) s.c. on the right hind leg of 6- to 8-week-old female nude mice. On day 30 after

[6] Q. Zhang, C. Liang, Y.A. Yu, N. Chen, T. Dandekar, A.A. Szalay, unpublished data.

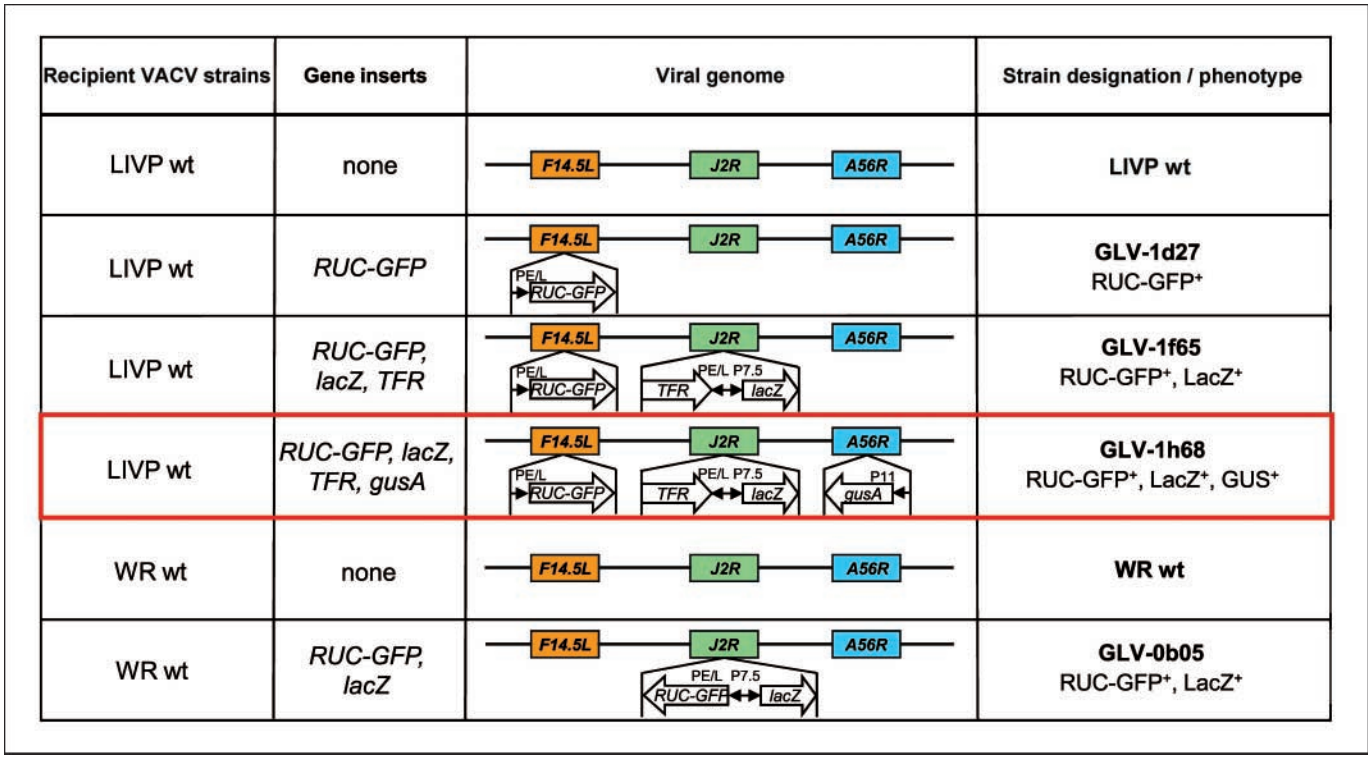

Figure 1. VACV constructs and marker genes. The wt LIVP was used for the generation of modified VACV with designations of GLV-1d27, GLV-1f65, and GLV-1h68. The wt VACV strain WR was used for the construction of GLV-0b05 virus. *P11,* VACV late P11 promoter; *PE/L,* VACV synthetic early/late promoter; *P7.5,* VACV early/late promoter.

cell implantation, a single dose of virus (5×10^6 pfu of GLV-1h68 in 100 μL PBS) was delivered via the femoral vein. Four mice per group were killed 3 and 6 weeks after GLV-1h68 injection. An identical number of control mice treated with PBS alone were killed in parallel. Total RNA was extracted from excised tumors using a QIAGEN RNeasy Protect Mini kit. Each RNA sample was eluted into 50 μL of DEPC-treated H_2O with addition of 2 μL of RNase inhibitor (Invitrogen) for storage at −80°C. Four tumor RNA samples from control animals sacrificed at the same time point were pooled together as reference after RNA isolation. Five micrograms of total RNA were amplified into cRNA and hybridized onto GeneChip Mouse Genome 430 2.0 arrays consisting of 45,000 probe set using GeneChip One-Cycle Target Labeling and Control Reagents (Affymetrix) according to manufacturer's instructions. Species-specific hybridization was tested by hybridizing in identical conditions amplified cRNA to the Human Genome U133 Plus 2.0 Array (Affymetrix).

Statistical analysis. Statistical analyses were done with SPSS, version 10 (SPSS, Inc.). The comparisons among treatment groups were made by ANOVA, and the differences between different groups were analyzed with LSD test when the ANOVA showed an overall significance. Statistical analysis of survival time was assessed using the log-rank test. P values of <0.05 were considered significant.

Array data analysis used the BRB array tool[7] developed by Dr. Richard Simon and Amy Peng Lam at NIH. Data were filtered at intensity of >10, excluding absent calls and normalized via median centering. Probes with missing value or notations with absent calls in >50% of the entire experiments were also excluded. Class comparison was adopted to identify genes differentially expressed at 3 or 6 weeks compared with the corresponding control samples. Differentially expressed genes were defined by univariate test ($P < 0.005$), false discovery rate (FDR < 0.12), and fold change (≥2). Selected genes were then further processed with Gene Ontology[8] to evaluate observed overexpected gene contributions within predetermined functional categories.

Results

GLV-1h68 retains its replication capacity in GI-101A cells. Schematic diagrams of wt LIVP and its derivatives used in this study are shown in Fig. 1. To examine whether insertions in the *F14.5L, J2R*, or *A56R* locus affected the infectivity and replication of individual recombinant viruses, infection studies were carried out using wt, single, double, and triple mutant LIVP viruses. Replication was determined in both dividing and resting CV-1 cells and in human breast tumor GI-101A cells. Compared with wt LIVP, all LIVP derivatives showed comparable replication in dividing CV-1 cells, but were approximately one-fifth as efficient in resting CV-1 cells 96 h after virus inoculation (Fig. 2*A*). Similarly, in GI-101A cells the infection and replication of LIVP mutant viruses were not very different from those of wt LIVP, suggesting that the single, double, or triple insertions within the LIVP genome did not detrimentally affect the entry and replication of the virus in CV-1 or GI-101A cells. In MEFs, however, the replication capacity of LIVP mutant viruses was greatly reduced or diminished compared with its wt strain.

Comparison of distribution of VACV strains in nude mice. Table 1*A* summarizes the virus distribution data in GI-101A tumor-bearing nude mice after i.v. injection of VACVs at a single dose of

[7] http://linus.nci.nih.gov/BRB-ArrayTools.html

[8] http://www.geneontology.org/

1×10^7 pfu per mouse. As shown in Table 1*A*, similar titers were recovered from the GI-101A tumors upon colonization with wt LIVP or its mutants. However, the systemic distribution data suggested that LIVP mutants were cleared more efficiently from the body than the wt virus. Compared with the distribution of wt LIVP and its derivatives, drastically elevated viral distribution was found in all organs of mice injected with wt WR. As high as 5.9×10^6 pfu of the virus per gram of tissue was found in the brain, and an even higher titer was recovered from the ovaries. Notable reduction in viral titer was achieved by using a virus with insertion into the TK gene in the WR genome (GLV-0b05), but still as high as 10^3 pfu of GLV-0b05 per gram of tissue was recovered from brain and 10^7 pfu of the virus per gram of tissue from ovaries. In contrast, both the brain and ovaries were found to be free of virus particles in mice injected with wt LIVP or its mutants.

GLV-1h68 shows remarkable safety profile in tumor-bearing nude mice. The toxicity of VACV infection on tumor-bearing nude mice was assessed by changes in body weight and macroscopic examinations of various organs (Fig. 2*B* and *C*). GI-101A tumor-bearing mice were i.v. injected with individual viruses at 1×10^7 pfu per mouse. Ten days after virus injection, significant weight loss (25%) was observed when wt WR was used as the inoculum. Mice injected with WR TK$^-$ or wt LIVP lost ~15% to 20% of their body weight 2 weeks after the injection. In contrast, no significant weight loss was noted when LIVP mutants were injected. These findings were in agreement with the viral distribution data and suggested that body weight loss might have been due to systemic infections of various organs by wt VACV.

Mice injected with wt WR or its TK$^-$ derivative exhibited 8-fold to 14-fold enlargement of ovaries compared with those in uninfected control mice (Fig. 2*C*). The viral titer recovered from ovary tissue 9 days after wt WR injection was 4.1×10^7 pfu/g, ~2.5-fold above the viral titer found in the ovaries of mice treated with WR TK$^-$ insertional mutant (Table 1*A*). In contrast, mice treated with wt LIVP or its insertional mutant derivatives had normal-sized ovaries, and no virus was recovered from these ovaries. Therefore, ovarian infection by wt WR or WR TK$^-$ might have caused the enlargement of ovaries.

Surprisingly, whereas the spleen weight of the mice treated with WR strains was not significantly different from that of the PBS control, those injected with LIVP or its mutants showed visible increases in spleen weight (Table 1*B*). The spleen enlargement could not be explained by virus infection in spleen tissues because there were no LIVP mutants recovered from spleen 2 weeks after virus injection.

Effect of GLV-1h68 colonization on the survival of tumor-bearing nude mice. To investigate whether successive attenuation of wt LIVP virus affects the survival of GI-101A tumor-bearing nude mice, these mice were monitored continuously for 130 days after virus injection (Fig. 2*D*). All tumor-bearing mice injected with 10^7 pfu of wt WR died within 11 days after infection. Those injected with wt LIVP survived up to 35 days. The insertion of the RUC-GFP

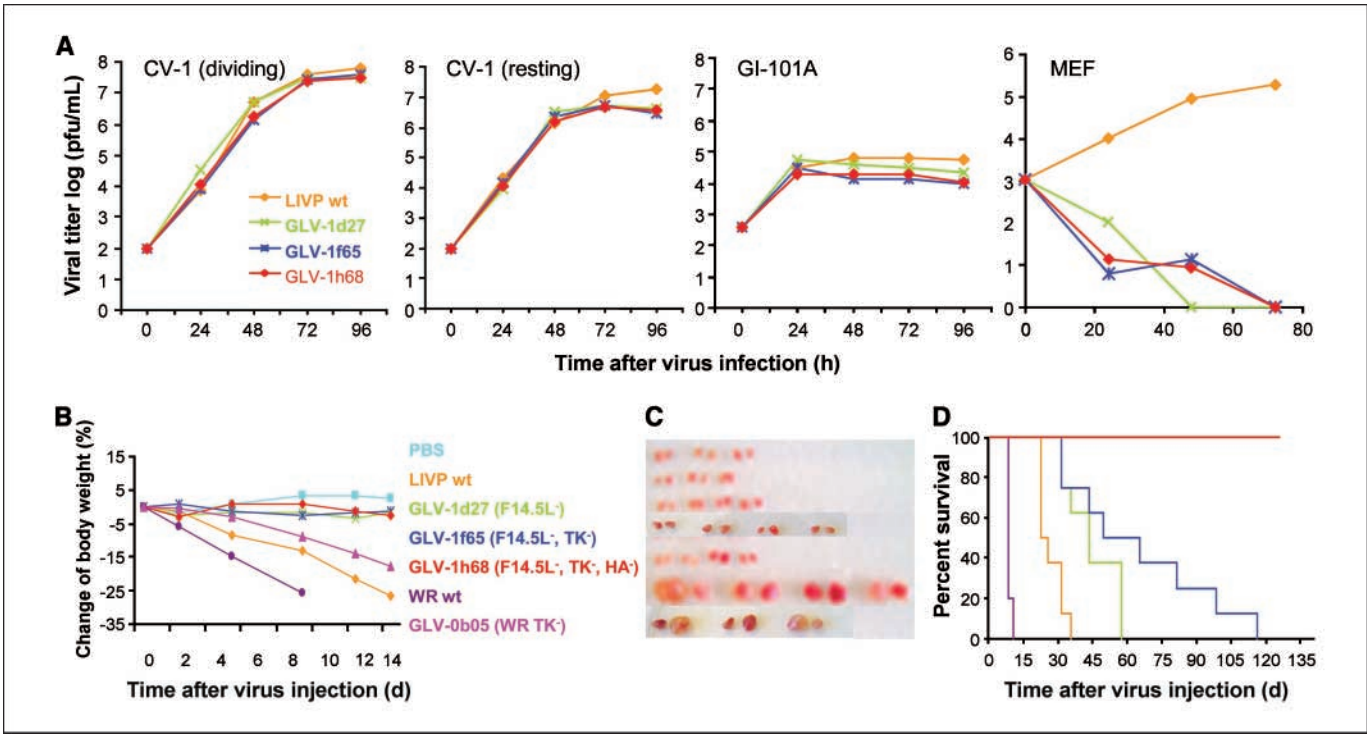

Figure 2. GLV-1h68 retains its replication capacity in tumor cells and shows a remarkable safety profile in tumor-bearing nude mice. *A,* viral replication in cell culture. CV-1 and GI-101A cells were inoculated with VACVs at MOI of 0.001 and MEFs at MOI of 0.01. The infected cells were harvested 24, 48, 72, or 96 h after infection. Viral titers were determined as pfu per ml of medium in duplicate by plaque assay in CV-1 cell monolayers. *B,* toxicity of VACV strains to mice with tumors. VACV strains were individually injected i.v. at single dose of 1×10^7 pfu in 100 μL PBS into mice with GI-101A (30 d old) tumors. Body weight was monitored twice a week thereafter. Change of body weight was calculated as $[(b' - t') - (b - t)]/(b - t)$, where b and t are the body weight and tumor weight on day of virus injection, respectively, and b' and t' are their corresponding weights on the day of monitoring ($n = 4$). The color coding for each virus also applies to *C* and *D*. *C,* effect of VACV strains on ovaries in nude mice with breast tumors. Mice were killed 9 d (WR-injected) or 14 d (other viruses injected) after virus injection. The ovaries were removed and weighed, and photographic images were taken. Enlargement of ovaries were seen in mice injected with WR viruses, but not in mice injected with LIVP and its mutants. *D,* survival of GI-101A tumor-bearing nude mice after treatment with VACV strains. GI-101A tumor-bearing mice were i.v. injected with individual VACV strains at a single dose of 10^7 per mouse at 30 d after tumor cell implantation. The difference in survival of the mice treated with GLV-1h68 was statistically significant compared with those treated with all other viruses ($P < 0.0001$).

expression cassette in the *F14.5L* locus of the LIVP genome significantly attenuated the virus so that the virus-injected tumor-bearing mice survived up to 57 days. When the double mutant virus (with insertions in the *F14.5L* and TK loci) was injected, mice lived up to 116 days after virus injection. The triple mutant GLV-1h68 was the most attenuated and showed an outstanding safety profile, with 100% of the tumor-bearing mice injected with the virus surviving without ill effect for the duration of the study (130 days postinfection). More remarkably, GLV-1h68–treated mice exhibited tumor eradication or reduction, and no metastases were observed at the end of the study. On the other hand, the control mice injected with PBS had to be euthanized by day 57 due to excessive tumor burden, often accompanied by visceral metastases.

GLV-1h68 eradicates human breast tumor xenografts in nude mice. During the survival studies, we observed that GLV-1h68 caused a remarkable decrease in the size of human breast tumor xenografts in nude mice. Examination over time revealed that, after i.v. injection of the virus, breast tumors ($\sim$300–500 mm^3 initially) showed a three-phase growth pattern (Fig. 3*A*). In Phase I (growth phase), the size of tumors increased continually until they reached an aggregate volume of $\sim$1,500 to 2,000 mm^3. A slightly larger tumor volume was observed in this phase upon viral colonization compared with control mice with no virus infection. Fourteen days post–virus injection, tumor growth was arrested (Phase II, inhibitory phase) when compared with the uninfected control group. The inhibitory phase persisted for $\sim$2 weeks, followed by tumor regression. This regression phase (Phase III) then continued and resulted in complete tumor elimination in >95% of the mice within 130 days after virus injection.

The three-phase tumor progression pattern was observed when a single dose of 10^5, 10^6, or 10^7 pfu of GLV-1h68 was delivered through the tail or femoral veins, indicating that 10^5 pfu of virus was sufficient to achieve tumor colonization and therapeutic efficacy in nude mice. No release of infectious viral particles was found in the blood 14 days after virus injection or during subsequent tumor progression stages.

Tumor regression monitored by light extinction. In previous studies, we showed that viral titers in tumors could be estimated based on levels of luminescent and fluorescent light emission (24). In this study, virus-mediated light emission was used to monitor the progression of breast tumors that were colonized by GLV-1h68. Imaging data obtained during the three phases of tumor growth observed after virus injection is shown in Fig. 3*B*. Images obtained 14 days after virus infection (at end of Phase I) indicated a massive viral replication only within the tumor region. At the end of Phase II, $\sim$28 days postinfection, a significant reduction in tumor size was visible. This also corresponded with drastic reduction in GFP signal within regressing tumor tissue. In Phase III, 56 days after VACV injection, the photographic image showed a nearly complete regression of the implanted breast tumors, in parallel with complete light extinction in the same tumor region.

Table 1.

(*A*) Distribution of VACV in tissues of GI-101A tumor-bearing nude mice

Tissue	Median of viral recovery, pfu/g of tissue (n = 4)					
	WR wt*	GLV-0b05	LIVP wt	GLV-1d27	GLV-1f65	GLV-1h68
Brain	5.9×10^6	3.8×10^3	0	0	0	0
Kidneys	1.1×10^7	2.3×10^4	4.1×10^2	4.3×10^2	0	0
Lungs	1.7×10^6	2.2×10^3	1.7×10^2	1.3×10^3	8.0×10^2	7.7×10^2
Spleen	1.7×10^6	4.3×10^2	4.1×10^3	0	0	0
Ovaries	4.1×10^7	1.6×10^7	0	0	0	0
Bladder	1.1×10^4	0	0	0	0	0
Liver	2.6×10^5	8.6×10^3	3.5×10^3	0	2.3×10^2	0
Heart	6.3×10^4	4.3×10^2	0	0	0	0
Serum †	1.2×10^3	0	0	0	0	0
Tumor	3.0×10^9	5.9×10^8	1.1×10^9	1.0×10^9	4.9×10^8	1.0×10^9

(*B*) Relative spleen weight in mice with or without tumors after virus injection

	Relative spleen weight, ‡ mean ± SD (n = 4–8)						
	PBS	WR wt*	GLV-0b05	LIVP wt	GLV-1d27	GLV-1f65	GLV-1h68
No tumor	50.5 ± 11.2			48.0 ± 13.1			
GI-101A	84.1 ± 14.6	57.9 ± 10.9	73.1 ± 19.3	108.4 ± 39.4§	151.8 ± 27.9§	159.9 ± 22.7§	117.7 ± 15.3§

Note: Each mouse was inoculated with 10^7 pfu of virus, and unless specified otherwise, mice were sacrificed 14 d after virus injection.
*Mice were sacrificed 9 d after virus injection.
† pfu/20 μL of serum.
‡ Relative spleen weight = weight of spleen (g) × 10^4/[body weight (g) − tumor weight (g)].
§ $P < 0.05$ when compared with nonmarked groups (LSD test).

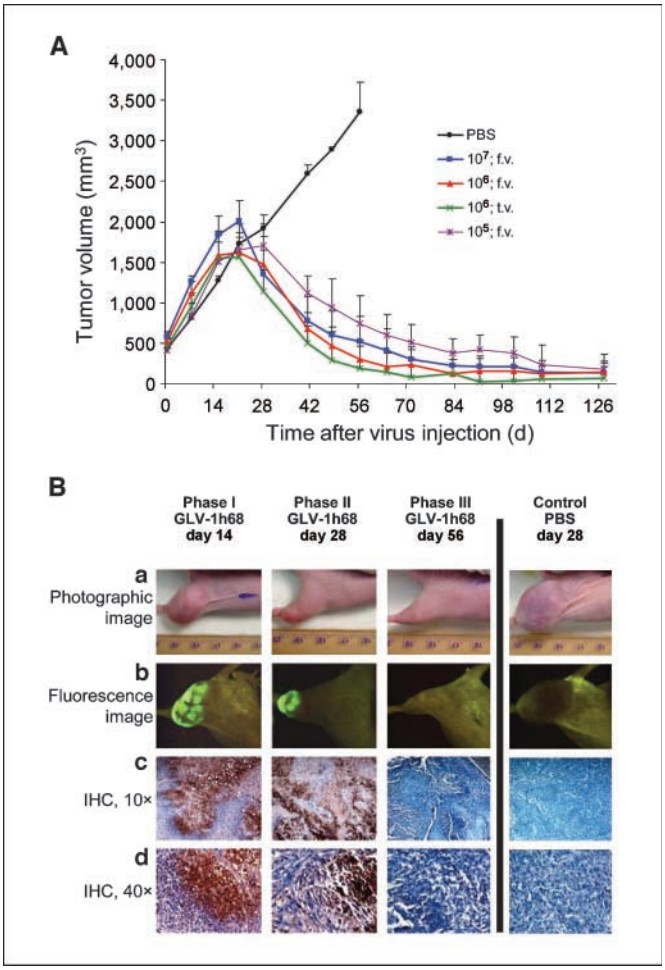

Figure 3. Characterization of tumor progression after virus injection. *A,* GLV-1h68 eliminates human breast tumors in nude mice. Mice with breast tumors (30 d old) were injected i.v. with GLV-1h68 virus at three different doses (10^5, 10^6, and 10^7 pfu/100 μL PBS per mouse) or with PBS as control. Tumor growth was monitored by measuring the tumor volume twice a week. *B,* monitoring of tumor and VACV elimination by light extinction in nude mice treated with GLV-1h68. Mice were i.v. injected with a single dose (1×10^7 pfu per mouse) of GLV-1h68 or PBS as control 30 d after breast tumor cell implantation. Bright field photographs (*a*) and fluorescence (*b*) images were taken 14, 28, and 56 d after virus or PBS injection. One representative mouse is presented. The data show a drastic reduction of tumor volume in mice injected with GLV-1h68. Two weeks after virus injection, strong fluorescence of GFP was seen in tumors with a volume of ~1400 mm^3. An additional 2 wk later, a much reduced GFP fluorescence was observed at tumor size of ~480 mm^3 in the same mouse. After 56 d, no GFP fluorescence was seen in the tumor which was ~180 mm^3 in size. *c* and *d,* immunohistochemical analyses of expression of GLV-1h68–encoded β-galactosidase in tumors excised from mice that were killed 14, 28, and 56 d after virus delivery. β-Galactosidase activity was detected concomitant with light emission and was completely eliminated as light emission was extinguished (at day 56). *c,* magnification, 10×. *d,* magnification, 40×.

These findings indicated strongly that, concomitantly with the elimination of breast tumor cells or tissues, the colonizing viral particles and the virus-encoded light-emitting proteins were also eliminated from the tumor site. Therefore, we were able to show the real-time monitoring of tumor regression based on light extinction.

The GLV-1h68–mediated β-galactosidase expression in regressing tumors was also analyzed with immunohistochemical staining. The presence of β-galactosidase (brown) in tumor sections 14 days after virus infection (Phase I) was shown in Fig. 3*B, c and d*. The immunohistochemical staining of β-galactosidase was also visible in the tumor section 28 days after virus infection. However, at end of Phase III, in parallel with extinction of GFP fluorescence, β-galactosidase staining from infected tumor section was completely absent. Neither GFP fluorescence nor β-galactosidase staining could be documented outside of tumor tissues or in uninfected tumors.

Host-specific transcriptional changes during tumor growth inhibition and regression. Affymetrix mouse arrays are relatively species specific.[9] Hence, genes identified in this study as differentially expressed may primarily represent host cells infiltrating the tumor. Previous work in our laboratory using human specific arrays did not identify significant changes in human xenografts at earlier time points after GLV-1h68 injection (20 h and 7 days). Significant alterations were noted at day 21 corresponding to the plateau of tumor growth and the beginning of the regression phase (data not shown). Thus, the analyses of host responses were limited to 3 and 6 weeks during the growth inhibition and the regression phases after viral injection. Host gene profiling analysis (F test) identified 681 differentially expressed genes at 3 and 6 weeks ($P < 0.005$; false discovery rate < 0.12; permutation $P < 0.05$), compared with corresponding control samples (Fig. 4*A* and Supplementary Table S1). Gene Ontology database was queried to assign genes to functional categories; expected (number of genes present in the array platform belonging to each category) versus observed (number of genes actually identified by the study belonging to each category) gene number for each respective category is reported. This approach pointed at major histocompatibility class I, chemokine receptor binding, chemokine activity, and cytokine activity as functional categories over represented among up-regulated genes in virus-injected mice (Fig. 4*B*). Peptidases, proteases, and other enzymatic function-related genes were preferentially down-regulated (Fig. 4*B* and Supplementary Table S1). Based on biological processes function, the analysis confirmed a predominance of host immune defense functions (Fig. 4*C*). To assess the changes of potential cross hybridization of human genes to the mouse chip, we hybridized amplified cRNA also to a Human Genome U133 Plus 2.0 Array and identified genes differentially expressed between control and treated samples. This analysis confirmed that fewer than 50% of the genes identified with the mouse arrays were differentially expressed according to the human chip, and among them, the few immune-related genes that resulted differentially expressed displayed very low fluorescence intensity in the human (<100) compared with the high or very high intensity displayed by the same genes in the mouse arrays (data not shown). This suggests that the same probes favor hybridization to mouse targets compared with the human targets. Histologic evaluation of control and treatment samples also supported a stronger peritumoral and intratumoral inflammatory infiltrate in treated samples (Fig. 5). Overall, it seems reasonable to conclude that a mouse-related immune response is part of the process leading to tumor regression. Evaluation of individual gene annotations suggested preferential activation of proinflammatory transcripts, such as chemokine ligands (*Ccl2, Ccl27–Ccl9, Ccl212, Cxcl9, Cxcl10, Cxcl12*), interleukin, and chemokine receptors (*Il13r, Il18,* and *Ccr2*). In addition, a panel of IFN-stimulated genes (*Ifi202b, Ifi203, Ifi204, Ifi205, Ifi35, Ifi44, Ifi47, Ifih1, Ifit1, Ifit2, Ifit3, Ifitm3, Igtp, Iigp1, Isgf3g*) were significantly induced in association

[9] http://www.affymetrix.com/support/technical/comparison_spreadsheets.affx

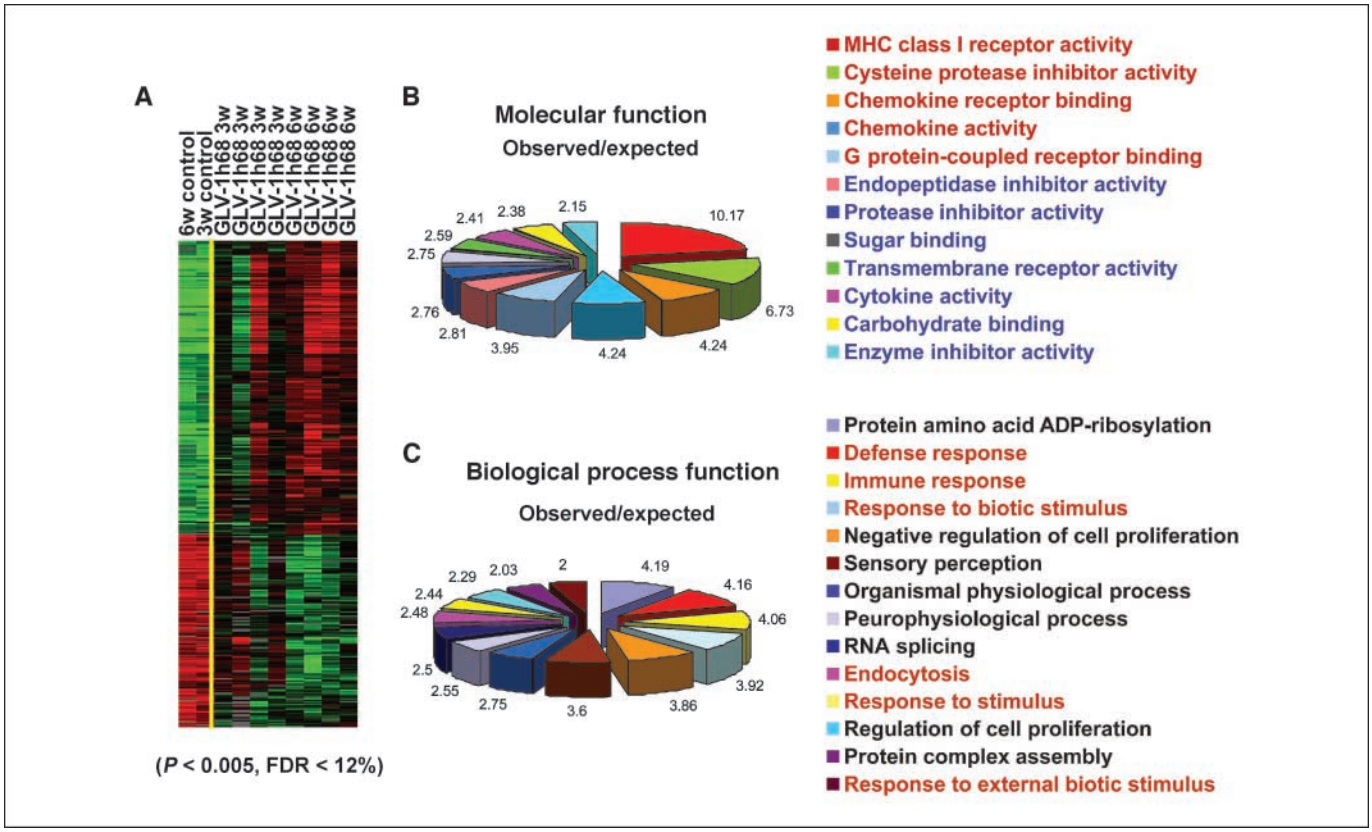

Figure 4. Host gene expression profiling analysis. *A,* supervised cluster visualization of differentially expressional genes among control, 3 and 6 wk post–virus injection (*F* test, $P < 0.005$, FDR < 0.12, and fold change ≥ 2). Heat map was generated using centralized $\log^2$ intensity (37). *B,* gene ontology expected versus observed gene analysis based on gene molecular function. Red labeled gene function group are up-regulated genes. *C,* gene ontology expected versus observed gene analysis based on biological processing function. Red labeled legends are gene groups with immunologic function and up-regulated.

with the up-regulation of *STAT-1* and IFN regulatory factor-7 (*Irf7*); the latter is strongly indicative of the activation of type I IFN pathways. Finally, genes denoting infiltration and activation of immune cells were observed, including *Cd69, Cd48, Cd52,* and *Cd53,* expressed on activated T cells, natural killer (NK) cells, macrophages, granulocytes, and dendritic cells and associated with leukocyte activation and NK cytolytic function.

Discussion

This paper describes the construction of a novel VACV, GLV-1h68, which carries three separate insertions in the *F14.5L, J2R* (TK), and *A56R* (hemagglutinin) loci of LIVP genome. We have documented that, whereas the triple insertions greatly reduced the replication of GLV-1h68 in normal mouse cells (e.g., MEF), the replication of GLV-1h68 in tumor cells (e.g., GI-101A) was not detrimentally affected. Injection (i.v.) of GLV-1h68 into nude mice with human breast tumor xenografts showed enhanced preference for colonization of tumors when compared with wt LIVP and WR strains. The differential colonization is reflected in the restricted distribution of GLV-1h68, mostly to tumors but not to other organs, and therefore resulted in less toxicity, allowing extended survival of tumor-bearing nude mice. Moreover, we discovered GLV-1h68 caused regression and complete elimination of human breast tumor xenografts in nude mice.

The regression of GI-101A tumor xenografts in mice by GLV-1h68 occurred in three phases. In Phase I, a slightly larger tumor was observed in the infected tumors compared with the uninfected control. This may be the result of an inflammatory response in tumors after viral infection (31) and/or expression of VGF by VACV after virus infection (32). The 3-fold to ~4-fold increase in tumor volume in both virus-treated and untreated mice suggested that the initial viral colonization did not seem to be sufficient to visibly interfere with tumor growth. The viral colonization and replication in tumors was shown through increasing light emission. Approximately 14 days after virus injection, the growth of GI-101A tumor xenografts was reduced and subsequently inhibited (Phase II), indicating that the oncolytic VACV GLV-1h68 started interfering with tumor growth, probably by massive oncolysis of tumor cells. In this inhibition phase, the number of lysed tumor cells was presumably equal to that of the dividing tumor cells. Phase II lasted for ~7 to 14 days. A constant level of fluorescence signal was also exhibited in this phase, indicating the balance between oncolytic activity and tumor cell infection. In contrast to Phase I and Phase II, at the initial stage of Phase III, a rapid tumor regression occurred, concomitantly with a gradual light extinction in tumors.

In previous studies, conventional chemotherapy treatments have been conducted in mice with subcutaneous GI-101A tumors.[10] Multiple doses of different agents, such as 5-fluorouracil, methotrexate, cyclophosphamide, and mitomycin-c, at different strengths were given i.v. into tumor-bearing mice. Treatment by methotrexate, cyclophosphamide, and mitomycin-c did show a

[10] Y.A. Yu, A. Aller, A.A. Szalay, unpublished data.

noticeable slowing of tumor growth 3 months after treatment; however, none of the chemotherapy regimens were able to shrink or eradicate the xenograft tumors. Therefore, the VACV-mediated tumor therapy clearly showed an advantage over traditional chemotherapy methods in nude mice bearing GI-101A tumors.

The fact that tumor-bearing nude mice successfully overcame infection by GLV-1h68 and survived the duration of the experiments suggests both considerable attenuation of the triple mutant of VACV and active involvement of the immune system. We believe that the one key factor that makes the successful elimination of tumors possible is the high attenuation status of GLV-1h68. This allowed the time for the virus to replicate and subsequent oncolysis to continue until tumor reduction and elimination. Wt WR, on the other hand, was lethal to mice before tumor regression or elimination could be completed. Although it is known that nude mice retain some residual T-cell activity (33) and antiviral cytotoxic T cells have been shown to play a crucial role in recovery from primary VACV infection, it is not clear how much residual T cells might have contributed to the clearance of GLV-1h68 in tumor-bearing nude mice. The involvement of the activated immune system is also suggested by the spleen enlargement observed in tumor-bearing mice infected with LIVP and its mutants. The spleen enlargement could not be explained by viral colonization of the spleen, because no LIVP mutants were recovered from spleens 2 weeks after i.v. injection. A likely explanation is that the LIVP viruses caused the tumor cells to lyse and that debris from the dying cells act locally or enter the circulation, producing extensive proinflammatory signals. In addition, cytokine and chemokine produced by the cancer cells stressed by the infections process may trigger a general immune response in the spleen and other lymphoid tissues, resulting in their enlargement.

Transcriptional analysis suggested that the host immune system may be involved in the process leading to the inhibition and regression phases of xenografts. Genes with immune function were incrementally enriched at tumor sites, particularly during the tumor regression phase (Fig. 4). These genes included cytokines, chemokines and their receptors, and a broad array of IFN-responsive genes. The up-regulation of *STAT-1*, IFN-regulated genes, and genes associated with immune cell migration/activation have all been previously described in humans in association with immune-mediated tumor rejection, acute allograft rejection, clearance of viral infection, and autoimmunity (34). Thus, transcriptional profiling supports the hypothesis that tumor regression after viral colonization is at least in part mediated through host defense mechanisms most likely belonging to the innate immune systems, because nude mice are deficient in T-cell and B-cell function. This conclusion is in accordance with a recent publication by Hicks et al. (35), suggesting that innate immunity plays a predominant role in the control of tumor growth. This notion is also supported by a recent study demonstrating that, indeed, VACV infection elicits a Toll-like receptor 2–mediated activation of the innate immune responses indirectly resulting in the predominant secretion of type I IFNs (36).

The latent induction of gene expression changes denote that the initiation of tumor rejection was mediated by viral replication. The production of proinflammatory cytokines, chemokines, and growth factors at the tumor site function as chemoattractants to recruit DC, monocytes, NK cells, and neutrophils and to trigger stroma cell infiltration. Activated infiltrating cells secrete more soluble proinflammatory molecules and promote cytolytic killing of tumor cells.

Based on the above findings, we therefore propose that the following mechanism may promote complete elimination of

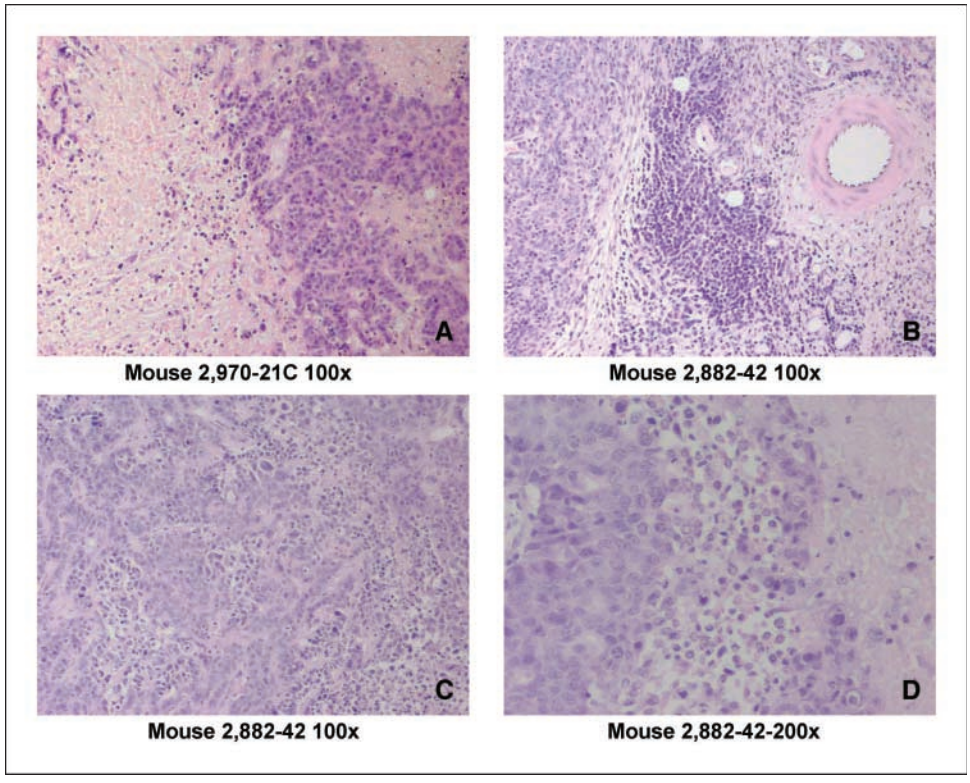

Figure 5. Representative example of inflammatory infiltrate in tumors from control mice (*A*) and mice that received GLV-1h68 injection (*B*, *C* and *D*). Tumors from virally injected mice displayed intense mononuclear cell infiltrates in peritumoral (*B*) and intratumoral (*C* and *D*) areas.

human breast tumor xenografts in nude mice. The first step requires reaching high viral titers (e.g., 1×10^9/g of tissue) in the tumor, which cause efficient oncolysis of tumor cells, followed by an inflammatory response. Upon continued massive lysis of tumor cells, proinflammatory signals are released, resulting in activation of the immune response. Subsequently, ongoing oncolysis, in combination with the elicited immune response, eliminates tumors from the mice. Ongoing experiments in our laboratory are designed to document the molecular events during this virus-mediated tumor elimination process. Unpublished data from our laboratory also indicate that the antitumoral effect of GLV-1h68 is not limited to GI-101A breast tumors. In summary, the light-emitting oncolytic virus GLV-1h68 may be viewed as a "live nanoparticle" or "live nanovector" with a natural tumor targeting, entry, and amplification capability and may be used as a simultaneous diagnostic and therapeutic vector for tumor treatment.

Acknowledgments

Received 1/11/2007; revised 7/18/2007; accepted 8/6/2007.

Grant support: Genelux Corporation (R&D facility in San Diego).

Conflict of interest: Q. Zhang, Y. Yu, N. Chen, and A. Szalay have financial interests in Genelux Corporation.

The costs of publication of this article were defrayed in part by the payment of page charges. This article must therefore be hereby marked *advertisement* in accordance with 18 U.S.C. Section 1734 solely to indicate this fact.

We thank Dr. T. Timiryasova for her valuable scientific and technical contributions, Dr. A. Aller for providing the GI-101A human breast carcinoma cell line, Ms. Jennifer Barb for her assistance with verifying the microarray data analysis, Dr. V. Hoffmann and Dr. L. Li for histologic imaging and evaluation, Mr. T. Trevino and Ms. R. Magpantay for excellent technical support, Dr. P. Hill for critical reading of the manuscript, Ms. A. Feathers for editorial support, and Mr. T. Hagood for help with graphics.

References

1. Coffin J, Varmus H, Hughes S, editors. *Retroviruses.* Cold Spring Harbor (NY): Cold Spring Harbor Press; 2000.
2. Talbot SJ, Crawford DH. Viruses and tumours-an update. Eur J Cancer 2004;40:1998–2005.
3. Heise CC, Williams AM, Xue S, Propst M, Kirn DH. intravenous administration of ONYX-015, a selectively replicating adenovirus, induces antitumoral efficacy. Cancer Res 1999;59:2623–8.
4. Grote D, Russell SJ, Cornu TI, et al. Live attenuated measles virus induces regression of human lymphoma xenographs in immunodeficient mice. Blood 2001;97: 3746–54.
5. Stojdl DF, Lichty BD, tenOever BR, et al. VSV strains with defects in their ability to shutdown innate immunity are potent systemic anticancer agents. Cancer Cell 2003;4:263–75.
6. Phuangsab A, Lorence RM, Reichard KW, Peeples ME, Walter RJ. Newcastle disease virus therapy of human tumor xenografts: antitumor effects of local or systemic administration. Cancer Lett 2001;172:27–36.
7. Pecora AL, Rizvi N, Cohen GI, et al. Phase I trial of intravenous administration of PV701, an oncolytic virus, in patients with advanced solid cancers. J Clin Oncol 2002;20:2251–66.
8. Norman KL, Coffey MC, Hirasawa K, et al. Reovirus oncolysis of human breast cancer. Hum Gene Ther 2002; 13:641–52.
9. Hirasawa K, Nishikawa SG, Norman KL, et al. Systemic reovirus therapy of metastatic cancer in immune-competent mice. Cancer Res 2003;63:348–53.
10. De Palma M, Venneri MA, Naldini L. *In vivo* targeting of tumor endothelial cells by systemic delivery of lentiviral vectors. Hum Gene Ther 2003;14:1193–206.
11. Fu X, Zhang X. Potent systemic antitumor activity from an oncolytic herpes simplex virus of syncytial phenotype. Cancer Res 2002;62:2306–12.
12. Nakamori M, Fu X, Pettaway CA, Zhang X. Potent antitumor activity after systemic delivery of a doubly fusogenic oncolytic herpes simplex virus against metastatic prostate cancer. Prostate 2004;60:53–60.
13. Shafren DR, Au GG, Nguyen T, et al. Systemic therapy of malignant human melanoma tumors by a common cold-producing enterovirus, coxsackievirus a21. Clin Cancer Res 2004;10:53–60.
14. Tseng JC, Levin B, Hurtado A, et al. Systemic tumor targeting and killing by Sindbis viral vectors. Nat Biotechnol 2004;22:70–7.
15. Vaha-Koskela MJV, Kallio JP, Jansson LC, et al. Oncolytic capacity of attenuated replicative semliki forest virus in human melanoma xenografts in severe combined immunodeficient mice. Cancer Res 2006;66: 7185–94.
16. Agrawal N, Bettegowda C, Cheong I, et al. Bacteriolytic therapy can generate a potent immune response against experimental tumors. Proc Natl Acad Sci U S A 2004;101:15172–7.
17. Zhao M, Yang M, Li XM, et al. Tumor-targeting bacterial therapy with amino acid auxotrophs of GFP-expressing *Salmonella typhimurium*. Proc Natl Acad Sci U S A 2005;102:755–60.
18. Puhlmann M, Brown CK, Gnant M, et al. Vaccinia as a vector for tumor-directed gene therapy: Biodistribution of a thymidine kinase-deleted mutant. Cancer Gene Ther 2000;7:66–73.
19. McCart JA, Ward JM, Lee J, et al. Systemic cancer therapy with a tumor-selective vaccinia virus mutant lacking thymidine kinase and vaccinia growth factor genes. Cancer Res 2001;61:8751–7.
20. Shida H, Hinuma Y, Hatanaka M, et al. Effects and virulences of recombinant vaccinia viruses derived from attenuated strains that express the human T-cell leukemia virus type I envelope gene. J Virol 1988;62:4474–80.
21. Lattime EC, Lee SS, Eisenlohr LC, Mastrangelo MM. *In situ* cytokine gene transfection using vaccinia virus vectors. Semin Oncol 1996;23:88–100.
22. Timiryasova TM, Chen B, Haghighat P, Fodor I. Vaccinia virus-mediated expression of wild-type p53 suppresses glioma cell growth and induces apoptosis. Int J Oncol 1999;14:845–54.
23. Kwak H, Horig H, Kaufman HL. Poxviruses as vectors for cancer immunotherapy. Curr Opin Drug Discov Devel 2003;6:161–8.
24. Yu YA, Shabahang S, Timiryasova TM, et al. Visualization of tumors and metastases in live animals with bacteria and vaccinia virus encoding light-emitting proteins. Nat Biotechnol 2004;22:313–20.
25. McCart JA, Mehta N, Scollard D, et al. Oncolytic vaccinia virus expressing the human somatostatin receptor SSTR2: molecular imaging after systemic delivery using ^{111}In-pentetreotide. Mol Ther 2004;10:553–61.
26. Rathinavelu P, Malave A, Raney SR, Hurst J, Roberson CT, Rathinavelu A. Expression of mdm-2 oncoprotein in the primary and metastatic sites of mammary tumor (GI-101) implanted athymic nude mice. Cancer Biochem Biophys 1999;17:133–46.
27. Timiryasova TM, Yu YA, Shabahang S, Fodor I, Szalay AA. Visualization of vaccinia virus infection using the renilla-luciferase-GFP fusion protein. In: Case JF, Herring PJ, Robison BH, Haddock SHD, Kricka LJ, Stanley PE, editors. Proceeding of the 11th International Symposium on Bioluminescence & Chemiluminescence. River Edge (NJ):World Scientific Publishing Co. pte. Ltd; 2000. p. 457–60.
28. Chakrabarti S, Sisler JR, Moss B. Compact, synthetic, vaccinia virus early/late promoter for protein expression. Biotechniques 1997;23:1094–7.
29. Flexner C, Broyles SS, Earl P, Chakrabarti S, Moss B. Characterization of the human immunodeficiency virus *gag/pol* gene products expressed by recombinant vaccinia viruses. Virology 1988;166:339–49.
30. Joklik WK. The purification of four strains of poxvirus. Virology 1962;18:9–18.
31. Bell JC, Lichty B, Stojdl D. Getting oncolytic virus therapies off the ground. Cancer Cell 2003;4:7–11.
32. Buller RM, Chakrabarti S, Moss B, Fredrickson T. Cell proliferative response to vaccinia virus is mediated by VGF. Virology 1988;164:182–92.
33. Silobrcic V, Zietman AL, Ramsay JR, Suit HD, Sedlacek RS. Residual immunity of athymic NCr/Sed nude mice and the xenotransplantation of human tumors. Int J Cancer 1990;45:325–33.
34. Mantovani A, Romero P, Palucka KA, Marincola FM. Tumor immunity: effector response to tumor and the influence of the microenvironment. The Lancet. In press.
35. Hicks AM, Riedlinger G, Willingham MC, et al. Transferable anticancer innate immunity in spontaneous regression/complete resistance mice. Proc Natl Acad Sci U S A 2006;103:7753–8.
36. Zhu J, Martinez J, Huang X, Yang Y. Innate immunity against vaccinia virus is mediated by TLR2 and requires TLR-independent production of IFN-β. Blood 2007;109: 619–25.
37. Ross DT, Scherf U, Eisen MB, et al. Systematic variation in gene expression patterns in human cancer cell lines. Nat Genet 2000;24:227–35.